Hydrodynamic model for second-harmonic generation at conductor surfaces with continuous profiles

J. A. Maytorena
Facultad de Ciencias, Universidad Autónoma del Estado de Morelos, Avenida Universidad 1001, 62210 Cuernavaca, Morelos, Mexico

W. Luis Mochán
Instituto de Física, Universidad Nacional Autónoma de México, Apartado Postal 139-B, 62191 Cuernavaca, Morelos, Mexico

Bernardo S. Mendoza
Centro de Investigaciones en Optica, Apartado Postal 948, 37000 León, Guanajuato, Mexico
(Received 5 July 1994)

We develop a hydrodynamic model for the calculation of second-harmonic generation (SHG) at the surface of conductors with arbitrary equilibrium electronic density profiles $n_0(r_\perp)$. We apply our model to simple profiles and calculate the linear surface conductivity $s(\omega)$ and the nonlinear surface susceptibility tensor $\chi_2^s(2\omega = \omega + \omega)$ for all ω, and we obtained the way they scale with the relevant bulk and surface parameters. The conductivity $s(\omega)$ displays a peak that corresponds to the dipolar surface plasmon at a frequency ω_d, which depends on the profile shape and width. The susceptibility $(\chi_2^s)_{\perp\perp\perp}$ has very large resonances at ω_d and $\omega_d/2$. The SHG efficiency is enhanced by several orders of magnitude at these resonances, suggesting that SHG spectroscopy might be a useful probe of surface collective modes.

I. INTRODUCTION

Optical spectroscopies of surfaces have the advantage of being nondestructive and of having a very good energy resolution. Furthermore, they may be employed to probe surfaces in any transparent ambient and they do not require ultrahigh vacuum. However, their use is hindered by the large penetration depth of electromagnetic waves at optical wavelengths. Procedures are required to disentangle the surface from the bulk contributions to the radiated light. In some instances this separation might be performed taking advantage of the reduced symmetry of most systems at their surface.[1] Second-harmonic generation (SHG) by centrosymmetric crystals has been proposed as a useful tool to study surfaces since their dipolar bulk contribution is suppressed by symmetry.[2] However, there is a residual bulk contribution originated from the small nonuniformity of the electric field and it is expected to be of a similar order of magnitude as the surface contribution, namely, a factor $(a/\lambda)^2$ smaller than for non-centro-symmetric materials, where a is a distance of the order of atomic dimensions and λ is the wavelength. To distinguish surface from bulk contributions some experiments have concentrated on the anisotropy of the signal,[3,4] and only a few have considered its frequency dependence.[5] Recently, experiments performed on metals immersed in an electrolyte[6] have shown that the surface contribution to SHG depends on the surface electronic distribution. Since a local theory of SHG (Ref. 7) yields no electronic density profile dependence,[8] spatial dispersion has to be accounted for.

There are different theoretical approaches in the literature to study SHG. Sipe *et al.*[9] have developed a phenomenological analysis of the surface and bulk susceptibility tensors, identifying their independent components, and the possible functional dependence of the second-order reflectance on the incidence and azimuthal angles for different crystal surfaces; they studied the possibility of separating the surface and bulk contributions using symmetry arguments, but they did not attempt actual calculations of the susceptibility. The nonlinear surface response was estimated[7,10] and later calculated[11,12] within the hydrodynamic model (HD) and microscopic calculations for simple metals have been performed using self-consistent jellium models.[13–15] Schaich and Mendoza[16] have developed a model that accounts for local field and crystallinity effects in the response of insulators and semiconductors,[17,18] and it has been extended to noble metals.[19] However, there are still very few attempts[20] to calculate the nonlinear spectra for more realistic models.

Early works[21] on the applicability of the HD model to the calculation of surface plasmon dipersion warned against its use since it yields spurious collective modes originated in the exponentially decaying tail of the electron gas density profile;[22] they recomended the use of less realistic profiles which go to zero at some well defined point. In spite of this and of other well known limitations such as the absence of Landau damping, the HD model has proved useful due to its relative simplicity which allows the study of systems which are more intricate than the simple semi-infinite jellium[19,23] and to bring forth a qualitative picture about the physics involved.

Previous hydrodynamic calculations[11,12] have been re-

stricted to discontinuous step profiles, and require that additional boundary conditions be imposed at the density discontinuities. Microscopic calculations of the nonlinear phenomenological parameter[24] $a(\omega)$ have been performed within the time-dependent local density approximation (TDLDA) and the random phase approximation (RPA),[14,15] and they display a very sensitive dependence on the details of the ground-state surface density profile; in particular, that $a(\omega = 0)$ is significantly larger[14,4] than in the previous hydrodynamic calculations.[11,12] However, these self-consistent calculations have been confined to the region $\omega < \omega_p/2$ due to technical difficulties whenever a propagating bulk plasmon at 2ω is excited. Chizmeshya and Zaremba[25] have extended the hydrodynamic model to account approximately for exchange and correlation employing in its formulation a gradient-corrected energy functional, and performed a self-consistent calculation. They calculated a in the static limit $\omega = 0$ only, and their results agreed with TDLDA.[13] We remark that low frequency experiments are frequently interpreted in terms of $a(0)$,[4] which dominates the angular dependence of SHG.[14]

In this paper, we apply the HD model to arbitrary surface density profiles and we calculate the nonlinear surface response and the SHG efficiency for all frequencies. The structure of the paper is the following: In Sec. II, we develop the hydrodynamic model to first and second order in a perturbing external field for inhomogeneous conductors starting from the equations of continuity and of momentum conservation. The boundary conditions obeyed by the induced first- and second-order polarization are obtained from the HD equations themselves. We also obtain scaling laws for the first- and second-order surface response. In Sec. III, we present a calculation of the linear and nonlinear surface response and of the SHG efficiency calculated for conductors with different surface profiles, and we discuss our results and compare them to those of earlier workers. We show that large resonant structures are to be expected in the SHG spectra at the multipolar surface plasmon frequencies and their subharmonics, suggesting an optical approach to the observation of these modes. Finally, Sec. IV is devoted to conclusions.

II. THEORY

Let us consider a p-polarized plane wave of frequency ω incident at an angle θ on a metallic surface which we represent as a semi-infinite jellium. The second-order induced currents are the sources of reflected p-polarized radiation of frequency 2ω generated with efficiency given by[24,11,26]

$$R_2(\omega) = \frac{8\pi e^2}{m^2\omega^2 c^3}\,|r(\omega)|^2\,, \tag{1}$$

$$r(\omega) = \frac{1}{8}\frac{\omega^2}{\Omega^2(\omega)}\epsilon(\omega)[\epsilon(\omega)-1]t_p(2\omega)t_p^2(\omega)\tan\theta \times\left[a(\omega)\frac{\epsilon(2\omega)}{\epsilon(\omega)}\sin^2\theta - b(\omega)\frac{2\eta(\omega)\eta(2\omega)}{\epsilon(\omega)}\cos^2\theta + 2d(\omega)\frac{\Omega^2(\omega)}{\Omega^2(2\omega)}\right], \tag{2}$$

where

$$\Omega^2(\omega) = \omega(\omega + i/\tau), \tag{3}$$

$$\eta(\omega) = [\epsilon(\omega) - \sin^2\theta]^{1/2}/\cos\theta, \tag{4}$$

$$t_p(\omega) = 2/[\epsilon(\omega) + \eta(\omega)], \tag{5}$$

$\epsilon(\omega) = 1 - \omega_b^2/\Omega^2(\omega)$ is the transverse dielectric function, $t_p(\omega)$ is the Fresnel transmission coefficient for p polarization, τ is a phenomenological damping parameter, $\omega_b = (4\pi n_b e^2/m)^{1/2}$ is the bulk plasma frequency, n_b is the bulk equilibrium electron density, $-e$ and m the electron charge and mass, and c the speed of light.

The dimensionless functions $a(\omega)$ and $b(\omega)$ parametrize the surface SHG response, while the bulk contribution is characterized by $d(\omega)$.[24,11] It is known that $b(\omega) = -1$ and $d(\omega) = 1$ independently of frequency for a flat jellium.[11,7] Therefore, in this work we shall concentrate on $a(\omega)$, which we write in terms of the nonlinear susceptibility $(\chi_2^s)_{\perp\perp\perp}(2\omega = \omega + \omega)$ as[12]

$$(\chi_2^s)_{\perp\perp\perp} = -\frac{a}{4en_b}\left[\frac{1-\epsilon}{4\pi\epsilon}\right]^2. \tag{6}$$

The susceptibility χ_2^s is defined through the response of the surface polarization to the field $E_j(0^-)$ just outside of the metal,

$$(P_2^s)_i \equiv (\chi_2^s)_{ijk}E_j(0^-)E_k(0^-). \tag{7}$$

Since we are interested in the surface region's response, and we assume that the selvedge's width is much less than an optical wavelength, we may perform our calculation in the non-retarded regime and ignoring the field variations along the surface.[12] We start our HD calculation from the continuity equation and from Euler's equation for momentum conservation in a semi-infinite electron fluid of density $n(z,t)$ and velocity field $u(z,t)\hat{z}$ in the presence of an electric field $E(z,t)\hat{z}$, where we take the z direction along the surface normal,

$$\partial_t n + \partial_z(nu) = 0, \tag{8}$$

$$mn\partial_t u + mnu/\tau + mnu\partial_z u = -neE - \partial_z p(n). \tag{9}$$

The consecutive terms of Eq. (9) correspond to inertial forces, dissipation through friction with the positive background, convective momentum flow, electric force and a pressure gradient. We calculate the pressure p starting from the density dependence of the average energy of a fermion within a noninteracting homogeneous gas $U/N = \frac{9}{10}\gamma n^{2/3}$, where $\gamma = (3\pi^2)^{2/3}\hbar^2/(3m)$. Then, assuming local equilibrium, the pressure is

$$p(n) = n^2\frac{\partial(U/N)}{\partial n} = \frac{3}{5}\gamma n^{5/3}(z,t), \tag{10}$$

as in the Thomas-Fermi theory. We account partially for the Coulomb interaction identifying E as the self-consistent mean field and we neglect exchange and correlation.[25]

Now we perturb the system by an external monochromatic field $D(z,t) = \mathrm{Re}(De^{-i\omega t})$ and expand all quantities such as n, u, etc., in powers of D. To zero order,

Eq. (9) yields

$$-en_0(z)E_0(z) = \partial_z p_0(z) = m\beta_0^2(z)\partial_z n_0(z), \quad (11)$$

where $\beta_0^2(z) = \frac{\gamma}{m} n_0^{2/3}(z)$. $E_0(z)$ plays the role of an effective field which confines the electron gas to a semispace, acting against the pressure term $p_0 = \frac{3}{5}\gamma n_0^{5/3}(z)$ leading to the the equilibrium density profile $n_0(z)$.

Now we expand Eqs. (8) and (9) to first order, and substitute Eq. (11) to obtain a differential equation for the first-order polarization P_1,

$$\frac{\gamma}{m} n_0(z)\partial_z\left[n_0^{-1/3}\partial_z P_1\right] + \beta_0^2(z)q_1^2(z)P_1 = S_1(z), \quad (12)$$

with a source term

$$S_1(z) = -\frac{\omega_p^2(z)}{4\pi} D, \quad (13)$$

where $\omega_p^2(z) = \omega_b^2 n_0(z)/n_b$ is the local plasma frequency, and

$$q_j^2(z) = \frac{\Omega^2(j\omega) - \omega_p^2(z)}{\beta_0^2(z)}, \quad j = 1, 2 \quad (14)$$

is the local plasmon wave number at the fundamental ($j = 1$) [or second-harmonic ($j = 2$)] frequency. In deriving Eq. (12), we employed the relation between electric current density $j = -enu$ and P, namely, $j = \partial_t P$, and we wrote the self-consistent field $E_1(z) = D - 4\pi P_1(z)$ in terms of the external and the depolarization fields.

Using a similar procedure, we obtain the following equation for the second-order polarization P_2 oscillating at the second harmonic 2ω,

$$\frac{\gamma}{m} n_0(z)\partial_z\left[n_0^{-1/3}\partial_z P_2\right] + \beta_0^2(z)q_2^2(z)P_2 = S_2(z), \quad (15)$$

whose source

$$S_2(z) = \frac{\gamma}{6me} n_0(z)\partial_z(n_0^{-2/3}\partial_z P_1)^2 - \frac{\omega^2}{en_0^2(z)} P_1^2(z)\partial_z n_0 + \frac{1}{2en_0(z)}(3\omega^2 + i\omega/\tau)\partial_z P_1^2 \quad (16)$$

arises from the spatial derivatives of the equilibrium density n_0 and from the square $P_1^2(z)$ of the linear polarization.

We remark that equations similar to our Eq. (12) have appeared repeatedly in the literature.[27] Calculations of surface plasmon dispersion relations[28,29] and of photoyield spectra[30] within an hydrodynamic approach have employed a modified form of Eq. (12) in which its first term is written as $\beta^2\partial_z^2 P_1$,[31] where $\beta^2 = C\frac{\gamma}{m}n_0^{2/3} = \frac{1}{3}Cv_F^2$. The constant $C = 1$ for $\omega\tau \ll 1$ and $C = \frac{9}{5}$ for $\omega\tau \gg 1$ in order to agree with the long wavelength limit of RPA in the bulk.[32] Although it is adequate in the bulk, this modified equation ignores the spatial derivatives[29,33] of n_0 and is inconsistent with the HD equations of motion close to the surface. In the present work, we have opted for consistency and written the equations directly as derived from the HD equations for the *inhomogeneous* electron gas. Sipe *et al.*[10] and Corvi and Schaich[11] have stated equations consistent with (12) and (15) but the former did not attempt an explicit solution and only made an order-of-magnitude estimate of a, and the latter solved them only for abrupt-step profiles. To our knowledge, ours is the first solution to the consistent HD first and second-order equations.

The second order differential equations (12) and (15) can be solved analytically in the bulk region where n_0 is independent of z,

$$P_1(z) = P_b + A_1 e^{iq_1 z}, \quad (17)$$

$$P_2(z) = A_2 e^{iq_2 z} + \frac{iq_1}{en_b\beta_b^2}\left(\frac{\nu_2 A_1^2}{q_2^2 - 4q_1^2} e^{2iq_1 z} - \frac{P_b\nu_1 A_1}{q_2^2 - q_1^2} e^{iq_1 z}\right), \quad (18)$$

and they can be integrated numerically near the surface where n_0 varies from 0 in vacuum to its bulk value n_b. Here, $\beta_b = \beta_0(\text{bulk})$, $\nu_1 = -\omega(3\omega + i/\tau)$, $\nu_2 = [8\omega^2 + 2i\omega/\tau + \omega_p^2(z)]/3$, $P_b = P_1(\text{bulk}) = [\epsilon(\omega) - 1]D/4\pi\epsilon(\omega)$ is the bulk polarization induced by a homogeneous external field and A_1 and A_2 are coefficients to be determined by sewing together the bulk and surface solutions using additional boundary conditions (ABC's). In the spirit of consistency within the HD model, as mentioned above, we derive the ABC's from the differential equations themselves. Therefore, we claim there is no ambiguity in the choice of ABC's. Demanding that the singularities that may be present on both sides of Eq. (12) should be of the same order leads immediately to the following linear ABC's:[34]

$$P_1 \text{ continuous}, \quad (19)$$

$$n_0^{-1/3}\partial_z P_1 \text{ continuous}. \quad (20)$$

These are equivalent to the ABC's first proposed by Forstmann and Stenschke[29] in order to satisfy energy and charge conservation at sharp boundaries between homogeneous layers. Similarly, from Eq. (15) it is possible to find the second-order ABC's,

$$P_2 \text{ continuous}, \quad (21)$$

$$\left(n_0^{-1/3}\partial_z P_2\right) - \frac{1}{6en_0^{2/3}}\left(n_0^{-1/3}\partial_z P_1\right)^2 - \frac{m\omega^2}{2e\gamma n_0^2} P_1^2 \text{ continuous}, \quad (22)$$

which are the same as those proposed in Ref. 12. After solving Eqs. (12) and (15) for $P_1(z)$ and $P_2(z)$ for a given profile $n_0(z)$, we calculate the surface polarizations,[35]

$$P_1^s \equiv \int dz[P_1(z) - P_1(\text{bulk})], \quad (23)$$

$$P_2^s \equiv \int dz P_2(z), \quad (24)$$

from which we identify the surface susceptibilities

$$(\chi_1^s)_{\perp\perp} = P_1^s/D, \tag{25}$$

$$(\chi_2^s)_{\perp\perp\perp} = P_2^s/D^2. \tag{26}$$

Finally, we obtain the linear surface conductivity[36]

$$s = -i\omega(\chi_1^s)_{\perp\perp} \tag{27}$$

and $a(\omega)$ [Eq. (6)]. It can be seen that for an abrupt profile, Eqs. (17) and (18) together with the boundary conditions (19)–(22) yield immediately the solution of Schaich and Liebsch.[12]

To find what the relevant parameters in our theory are, first we introduce a parameter z_s which is a measure of the *width* of the surface region, and we use it to normalize distance, i.e., $z \equiv z_s\tilde{z}$. Next, we normalize the ground-state density to its bulk value, $n_0(z) = n_b\tilde{n}_0(\tilde{z})$. Notice that $\tilde{n}_0(\tilde{z})$ contains information on the *shape* of the profile only. Finally, we use the bulk plasma frequency to normalize time; $\omega = \omega_b\tilde{\omega}$ and $\tau = \tilde{\tau}/\omega_b$. Performing these substitutions in Eqs. (12) and (15) it is straightforward to show that writing

$$P_1(z) = D\tilde{P}_1(\tilde{z}), \tag{28}$$

$$P_2(z) = D\frac{D}{en_bz_s}\tilde{P}_2(\tilde{z}); \tag{29}$$

we obtain differential equations whose coefficients depend *only* on the parameters $\tilde{\omega}$, $\tilde{\tau}$, and $\zeta_s \equiv z_s/\lambda_{\rm TF}$, where $\lambda_{\rm TF} = \beta_b/\omega_b$ is the Thomas-Fermi screening length. Therefore, for a given profile shape, the surface is entirely characterized within the HD model by the dimensionless parameter ζ_s. Since we have seen that $\tilde{P}_1(\tilde{z}) = \tilde{P}_1(\tilde{z};\tilde{\omega},\tilde{\tau},\zeta_s)$, $\tilde{P}_2(\tilde{z}) = \tilde{P}_2(\tilde{z};\tilde{\omega},\tilde{\tau},\zeta_s)$, then Eqs. (27), (6), and (1) yield $s = \beta_b\tilde{s}(\tilde{\omega},\tilde{\tau},\zeta_s)$, $a = \tilde{a}(\tilde{\omega},\tilde{\tau},\zeta_s)$, and $R_2 = [2/(n_bmc^3)]\tilde{R}_2(\tilde{\omega},\tilde{\tau},\zeta_s)$.

III. RESULTS

To illustrate our model we have chosen two simplified shapes for the equilibrium density profile $n_0(z)$ that interpolate between its vacuum and bulk values, namely, a linear profile,

$$\tilde{n}_0(\tilde{z}) = \begin{cases} 1, & \tilde{z} > 1 \\ \frac{1}{2}(1+\tilde{z}), & -1 < \tilde{z} < 1 \\ 0, & \tilde{z} < -1, \end{cases} \tag{30}$$

and a quadratic profile,

$$\tilde{n}_0(\tilde{z}) = \begin{cases} 1, & \tilde{z} > 1 \\ 1 - \frac{1}{2}(1-\tilde{z})^2, & 0 < \tilde{z} < 1 \\ \frac{1}{2}(1+\tilde{z})^2, & -1 < \tilde{z} < 0 \\ 0 & \tilde{z} < -1. \end{cases} \tag{31}$$

We will consider parameters that correspond roughly to K: we chose the bulk density parameter $r_s = 4.86a_0$ ($n_b \equiv 4\pi r_s^3/3$, a_0 is Bohr's radius), and we took $\omega_b\tau = 30$.[37] As discussed at the end of the previous section, our results can be easily scaled for different densities.

In Fig. 1, we show the real part of the linear conductivity $s(\omega)$ obtained from Eqs. (12), (23), (26), and (27) using both the linear and quadratic profiles. The conductivity $s(\omega)$ displays a peak at ω_b and a Lorentzian peak at a frequency ω_d which corresponds to the excitation of a dipolar surface plasmon. This collective mode appears in addition to the usual surface plasmon when the density profile is sufficiently diffuse. It was predicted by earlier hydrodynamic calculations of the surface plasmon dispersion[28,29,31] for several shapes of $n_0(z)$, and by calculations of the photoemission yield spectra for a two-step density profile.[30] Random phase approximation[37] and TDLDA calculations[38] for semi-infinite jellium also predict a similar resonance situated near $0.8\omega_b$. This multipole plasmon mode is suspected to be responsible for the large surface photoyield of Al,[39] and it has also been observed in the electron-energy-loss spectra (EELS) of smooth K and Na films,[40] although it is strongly shadowed by the regular (monopole) surface plasmon; for Al the dipolar mode is just too weak to be observable with EELS. Experiment has confirmed the position predicted through RPA and TDLDA.

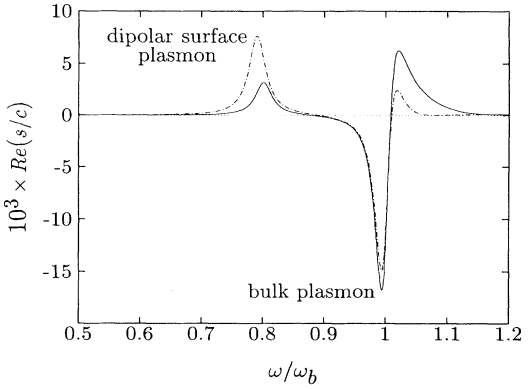

FIG. 1. Linear surface conductivity s calculated within the hydrodynamic model for K ($r_s = 4.86a_0$; for other metals the results scale with $1/r_s$) using a linear (dashed) and a quadratic (solid) surface profile, with a lifetime $\tau = 30/\omega_b$. The selvedge width $z_s = 3.5a_0$ ($z_s = 2.5a_0$) was fitted to the indicated position of the dipolar surface plasmon in the linear (quadratic) case.

Within our hydrodynamic model, the number of multipolar resonances, their position, and their strength depend on the width of the selvedge and on the shape of the density profile. Therefore, we have adjusted the width parameter z_s to locate the dipolar peak close to the expected frequency $\omega_d = 0.8\omega_b$, obtaining $z_s = 3.5a_0$ ($\zeta_s = 2.48$) for the linear profile and $z_s = 2.5a_0$ ($\zeta_s = 1.77$) for the parabolic one. Notice that for any other bulk density but the same surface profile shape, the position of the dipolar surface resonance depends only on ζ_s. The structure observed at $\omega = \omega_b$ corresponds to the excitation of the bulk plasmon. From $s(\omega)$ it is possible to obtain the surface impedance,[36] the reflection amplitude r_p, the surface plasmon dispersion relation, and the EELS spectrum. We have verified that our calculation yields a negative initial dispersion for the ordinary surface plasmon.[28,29,31,37]

So far, we have adjusted our model to reproduce qualitatively the main features of the surface linear

response.[27,37,38] In this way, we have exhausted the parameters of our model, so we proceed now to perform the nonlinear part of our calculation. In the following we calculate $a(\omega)$ and $R_2(\omega)$.

We start with $a(\omega)$ in the static limit which, according to Eq. (1), determines the low frequency ($\omega \ll \omega_b$) nonlinear reflectance. Previous calculations employing the HD model for the one-step discontinuous profile yield $a(0) = -\frac{2}{9}$ independently of r_s and slightly larger values for a two-step profile.[13,41] Much bigger negative values [$a(0) \approx -7$ for K and -30 for Al] have been obtained employing TDLDA (Refs. 14, 4, and 41) and the generalized Thomas-Fermi Dirac (GTFD) approximation.[25] Our HD calculation for linear and quadratic profiles with ζ_s adjusted to ω_d yields $a(0) \simeq -2.8$ and $a(0) \simeq -9.0$, respectively, independently of r_s. Thus, our result for the parabolic profile is in good agreement with microsopic calculations for K, but it becomes too small for Al, and the linear profile results underestimate both extreme limits. By increasing the widths of our profiles within reasonable limits, we have been able to increase $a(0)$ for given r_s to agree with TDLDA. However, by adjusting $a(0)$ we shift ω_d towards the red and we get spurious higher order multipolar plasmons.

Now we turn our attention to the high frequency limit. It is possible to demostrate quantum mechanically that $a(\omega \to \infty) = -2$ independently of r_s.[42] The HD model with a single abrupt profile yields an incorrect limit $a(\omega \to \infty) = -\frac{4}{3}$. We have verified that when we smooth the profile introducing a finite ζ_s, our model attains the correct limit $a \to -2$ for high enough frequencies. The smaller ζ_s, the higher the frequency of the asymptotic region. This limit has not been attained in the self-consistent calculations since they have been restricted to the range $0 \leq \omega \leq \omega_b/2$.

Figure 2 shows the numerically calculated frequency dependence of $a(\omega) \equiv |a(\omega)|e^{i\phi}$ for the two profiles for a fixed profile shape $\tilde{n}_0(\tilde{z})$ and lifetime parameter $\tilde{\tau}$, a depends only on $\tilde{\omega}$ and ζ_s and is independent of the bulk density. $a(\omega)$ displays large peaks at the dipolar plasmon frequency ω_d and at its subharmonic $\omega_d/2$, and at half the plasma frequency $\omega_b/2$ as could be anticipated. Our model does not include photoemission and, therefore, we did not obtain any structure related to the work function. For a discontinuous profile the HD model yields values of $a(\omega)$ of order $1-10$. We obtained at the resonance frequencies an enhancement of one to two orders of magnitude for the linear profile. For the quadratic profile $a(\omega)$ is enhanced up to four orders of magnitude. The resonance in $a(\omega)$ at the subharmonic of the surface collective mode was obtained previously in Ref. 15 employing TDLDA and RPA. Their results for K are bracketed by ours: with the linear profile we underestimate the peak by a factor of three, while we overestimate it by a factor of ten with the quadratic profile. For Al, our result for the linear profile agrees with the microscopic calculations and for the quadratic one it is too large by a factor of thirty.

We remark that the peak in the surface nonlinear response at ω_d has not been reported previously. The TDLDA and RPA calculations have been impeded for

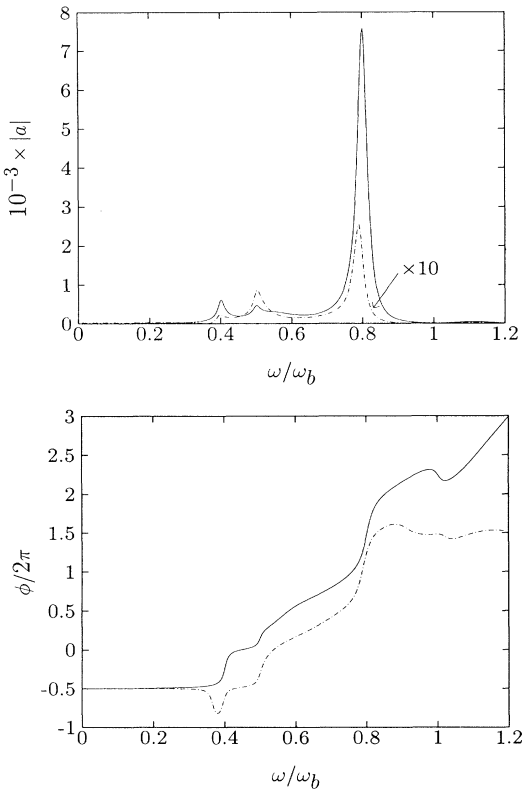

FIG. 2. Absolute value (upper panel) and phase (lower panel) of the nonlinear response function $a(\omega) = |a|e^{i\phi}$ calculated for a linear (dashed) and a quadratic (solid) surface profile. The parameters are as in Fig. 1.

$\omega > \omega_b/2$ by the propagation of a bulk plasmon at 2ω. On the other hand, since we use an analytical expression (18) for the polarization in the bulk region where the profile is constant, the propagation of plasmons produces no particular difficulties for our calculation.

In Fig. 3, we display the nonlinear efficiency for our two profiles calculated for p polarized light incident at

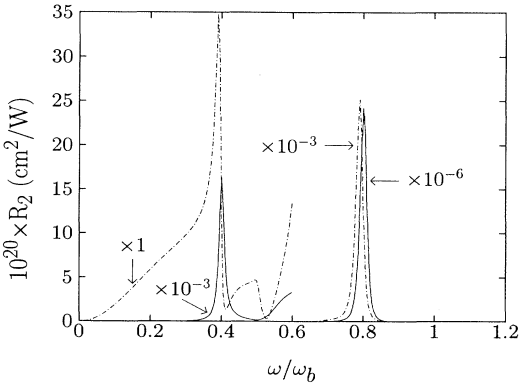

FIG. 3. Second-harmonic generation efficiency $R_2(\omega)$ calculated for a linear (dashed) and a quadratic (solid) surface profile. The angle of incidence $\theta = 60°$ and the other parameters are as in Fig. 1.

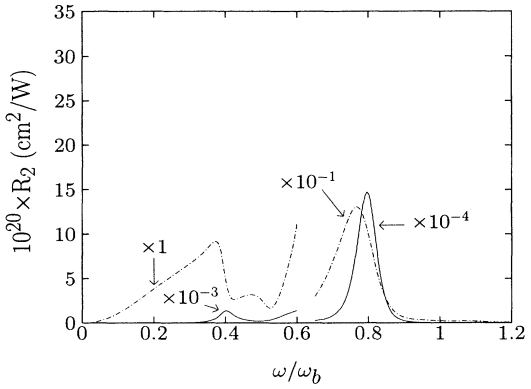

FIG. 4. Second-harmonic generation efficiency $R_2(\omega)$ calculated for a linear (dashed) and a quadratic (solid) surface profile. The angle of incidence $\theta = 60°$, the lifetime $\tau = 10/\omega_b$ and the other parameters are as in Fig. 1.

$\theta = 60°$ on a K surface and plotted using common units. Recall that for other metals our results scale with r_s^3. The results display a small structure at $\omega_b/2$ and two large peaks at $\omega_d/2$ and ω_d. Comparing our results to the hydrodynamic calculation shown in Fig. 2 of Ref. 11, we find the same order of magnitude in the regions out of resonance. However, the second-harmonic efficiency is increased by a large amount at resonance. For the linear profile the enhancement is about a factor of three at $\omega_d/2$ and three orders of magnitude at ω_d; for the quadratic profile the corresponding enhancements are three and six orders of magnitude. Our enhancements are larger than the peaks found in Ref. 11 for a two step profile.

We have performed similar calculations for different selvedge widths z_s and we have found that the resonances in R_2 track closely the peaks in the linear surface response s and their subharmonics, even for large widths for which several multipolar modes are present. This is in contrast to what was found in Ref. 11, where the peaks in R_2 seem not to be simply related to the multipolar surface modes.

To study the permanence of our results under increased dissipation, in Fig. 4 we display the nonlinear reflectance for a smaller lifetime $\omega_b\tau = 10$. The height of the multipolar resonance and that of its subharmonic are decreased by a large amount, but both peaks remain well defined and are clearly visible.

IV. CONCLUSIONS

In this paper, we have extended the hydrodynamic model to calculate the linear and second-order surface response and the SHG efficiency of semi-infinite metals taking account the presence of a continuous electronic density profile at their surface. It is known[21] that the hydrodynamic model is unable to deal with realistic profiles, since it overemphasizes the contributions to the response from the exponentially decaying tail. Therefore, in this paper, we employed two simple model profiles that interpolate between the bulk and vacuum. We chose the profile parameters so that the resonance frequency of the linear surface response fitted roughly the position of the dipolar surface collective mode, as obtained from self-consistent jellium calculations[37,38] and from experiment.[39,40]

We calculated the nonlinear susceptibility of K, and discussed its normal-to-the-surface component, characterized by the $a(\omega)$ parameter. We also calculated its nonlinear reflectance $R_2(\omega)$. We noticed that for a given profile shape, the surface is entirely characterized by its width in units of the Thomas-Fermi screening length, and we arrived at a set of simple scaling laws to extend our results to different metals.

We verified that our calculation of $a(\omega)$ has the correct asymptotic value at large frequencies and tends to underestimate its static value as compared with self-consistent jellium calculations,[15] although for the quadratic profile it yields good agreement in the case of K. The graphs of $a(\omega)$ and $R_2(\omega)$ display some structure at the subharmonic of the bulk plasma frequency, and very large peaks at the dipolar surface plasma frequency and its subharmonic. Peaks similar to the latter were also obtained in Ref. 15 and their height was bounded within our results for the linear and the quadratic profiles. There are no microscopic calculations above $\omega_b/2$. However, the kind of agreement we obtained with microscopic theories below $\omega_b/2$ gives us confidence that the huge peak at the dipolar surface plasmon is at least qualitatively correct.

These results suggest that the multipolar modes, which are difficult to observe in electron scattering experiments, might be observed through SHG spectroscopy. Usually, the experiments[3,4] have concentrated on the angular dependence of the SHG signal and there are few studies of the frequency dependence.[5,43] We hope our calculation encourages more experiments to measure the SHG spectra, and more theoretical calculations close to the surface resonances. In summary, the surface nonlinear susceptibility and its efficiency display a series of very large peaks corresponding to the excitation of multipolar surface plasmons, indicating that the observation of these elusive modes might be performed with SHG spectroscopy.

ACKNOWLEDGMENTS

This work was partially supported by DGAPA-UNAM under Project Nos. IN-102493 and 104594 and by CONACyT under Grant No. 3246-E9308.

[1] T. F. Heinz, in *Nonlinear Surface Electromagnetic Phenomena*, edited by H. E. Ponath and G. I. Stegeman (Elsevier, Amsterdam, 1991).

[2] N. Bloembergen, R. K. Chang, S. S. Jha, and C. H. Lee, Phys. Rev. **174**, 813 (1968); **178**, 1528(E)(1969); Y. R. Shen, *The Principles of Nonlinear Optics* (Wiley, New York, 1984); G. L. Richmond, J. M. Robinson, and V. L. Shannon, Prog. Surf. Sci. **28**, 1 (1988); Y. R. Shen, Nature (London) **337**, 519 (1989).

[3] For example, T. A. Driscoll and D. Guidotti, Phys. Rev.

B **28**, 1171 (1983); H. W. K. Tom, T. F. Heinz, and Y. R. Shen, Phys. Rev. Lett. **51**, 1983 (1983); D. A. Koos, V. L. Shannon, and G. L. Richmond, Phys. Rev. B **47**, 4730 (1993).

[4] R. Murphy, M. Yeganeh, K. J. Song, and E. W. Plummer, Phys. Rev. Lett. **63**, 318 (1989).

[5] L. E. Urbach, K. L. Percival, J. M. Hicks, E. W. Plummer, and H.-L. Dai, Phys. Rev. B **45**, 3769 (1992); K. J. Song, D. Heskett, H. L. Dai, A. Liebsch, and E. W. Plummer, Phys. Rev. Lett. **61**, 1380 (1988);

[6] P. Guyot-Sionnest, A. Tadjeddine, and A. Liebsch, Phys. Rev. Lett. **64**, 1678 (1990).

[7] J. E. Sipe and G. I. Stegeman, in *Surface Polaritons*, edited by V. M. Agranovich and D. L. Mills (North-Holland, Amsterdam, 1982).

[8] B. S. Mendoza and W. L. Mochan (unpublished).

[9] J. E. Sipe, D. J. Moss, and H. M. van Driel, Phys. Rev. B **35**, 1129 (1987).

[10] J. E. Sipe, V. C. Y. So, M. Fukui, and G. I. Stegeman, Phys. Rev. B **21**, 4389 (1980).

[11] M. Corvi and W. L. Schaich, Phys. Rev. B **33**, 3688 (1986).

[12] W. L. Schaich and A. Liebsch, Phys. Rev. B **37**, 6187 (1988).

[13] M. Weber and A. Liebsch, Phys. Rev. B **35**, 7411 (1987).

[14] A. Liebsch, Phys. Rev. Lett. **61**, 1233 (1988); **61**, 1897(E) (1988).

[15] A. Liebsch and W. L. Schaich, Phys. Rev. B **40**, 5401 (1989).

[16] W. L. Schaich and Bernardo S. Mendoza, Phys. Rev. B **45**, 14 279 (1992).

[17] Bernardo S. Mendoza, J. Phys. Condens. Matter **5**, A181 (1993).

[18] C. M. J. Wijers, Th. Rasing, and R. W. J. Hollering, Solid State Commun. **85**, 233 (1993).

[19] W. Luis Mochán and Bernardo S. Mendoza, J. Phys. Condens. Matter **5**, A183 (1993).

[20] A. V. Petukhov, Phys. Rev. B **42**, 9387 (1990); A. V. Petukhov and A. Liebsch, Surf. Sci. **294**, 381 (1993).

[21] P. Ahlqvist and P. Apell, Phys. Scr. **25**, 587 (1982); C. Schwartz and W. L. Schaich, Phys. Rev. B **26**, 7008 (1982).

[22] N. D. Lang and W. Kohn, Phys. Rev. B **1**, 4555 (1970).

[23] Shu Wang, Rubén G. Barrera, and W. Luis Mochán, Phys. Rev. B **40**, 1571 (1989); Shu Wang, W. Luis Mochán, and Rubén G. Barrera, *ibid.* **42**, 9155 (1990).

[24] J. Rudnick and E. A. Stern, Phys. Rev. B **4**, 4274 (1971).

[25] A. Chizmeshya and E. Zaremba, Phys. Rev. B **37**, 2805 (1988).

[26] V. Mizrahi and J. E. Sipe, J. Opt. Soc. Am. B **5**, 660 (1988); J. E. Sipe, *ibid.* **4**, 481 (1987).

[27] F. Forstmann and R. R. Gerhardts, *Metal Optics near the Plasma Frequency*, edited by G. Höhler, Springer Tracts in Modern Physics Vol. 109 (Springer, Berlin, 1986), Chaps. 2 and 3 and references therein.

[28] A. Bennett, Phys. Rev. B **1**, 203 (1970); S. DasSarma and J. J. Quinn, *ibid.* **20**, 4872 (1979); J. E. Sipe, Surf. Sci. **84**, 75 (1979).

[29] F. Forstmann and H. Stenschke, Phys. Rev. Lett. **38**, 1365 (1977); Phys. Rev. B **17**, 1489 (1978).

[30] K. Kempa and F. Forstmann, Surf. Sci. **129**, 516 (1983); C. Schwartz and W. L. Schaich, Phys. Rev. B **30**, 1059 (1984); K. Kempa and R. R. Gerhardts, Solid State Commun. **53**, 579 (1985).

[31] A. Eguiluz, S. C. Ying, and J. J. Quinn, Phys. Rev. B **11**, 2118 (1975); A. Eguiluz and J. J. Quinn, *ibid.* **14**, 1347 (1976); Phys. Lett. **53A**, 151 (1975).

[32] A. L. Fetter, Ann. Phys. (N.Y.) **81**, 367 (1973); A. D. Boardman, in *Electromagnetic Surface Modes*, edited by A. D. Boardman (Wiley, New York, 1982).

[33] S. Lundqvist, in *Theory of the Inhomogeneous Electron Gas*, edited by S. Lundqvist and N. H. March (Plenum, New York, 1983).

[34] M. del Castillo-Mussot, W. L. Mochán, and Bernardo S. Mendoza, J. Phys. Condens. Matter. **5**, A393 (1993).

[35] We are using the fact that in the unretarded limit $P_2(\text{bulk}) = 0$, so that the integral $P_2^s = \int P_2(z)dz$ is well defined. This implies that the second-harmonic charge induced at the surface is zero.

[36] W. Luis Mochán, R. Fuchs, and R. G. Barrera, Phys. Rev. B **27**, 771 (1983).

[37] P. J. Feibelman, Prog. Surf. Sci. **12**, 287 (1982); Phys. Rev. B **40**, 2752 (1989); K.-D. Tsuei, E. W. Plummer, and P. J. Feibelman, Phys. Rev. Lett. **63**, 2256 (1989).

[38] A. Liebsch, Phys. Rev. B **36**, 7378 (1987); K. Kempa, A. Liebsch, and W. L. Schaich, *ibid.* **38**,12 645 (1988).

[39] H. Levinson, E. W. Plummer, and P. J. Feibelman, Phys. Rev. Lett. **43**, 952 (1979).

[40] K.-D. Tsuei, E. W. Plummer, A. Liebsch, K. Kempa, and P. Bakshi, Phys. Rev. Lett. **64**, 44 (1990); K.-D. Tsuei, E. W. Plummer, A. Liebsch, E. Pehlke, K. Kempa, and P. Bakshi, Surf. Sci. **247**, 302 (1991).

[41] For a table of $a(\omega = 0)$ for several r_s calculated with different approaches see Ref. 15.

[42] B. S. Mendoza and W. L. Schaich, Bull. Am. Phys. Soc. **36**, 768 (1991).

[43] C. D. Hu, Phys. Rev. B **40**, 7520 (1989).